EPJ Web of Conferences **130**, 05004 (2016) DOI: 10.1051/epjconf/201613005004
MESON 2016

Measurement of hadron cross sections with the SND detector

V. P. Druzhinin[1,2,⋆], M. N. Achasov[1,2], A. Yu. Barnyakov[1,2], K. I. Beloborodov[1,2], A. V. Berdyugin[1,2], A. G. Bogdanchikov[1], A. A. Botov[1], T. V. Dimova[1,2], V. B. Golubev[1,2], L. V. Kardapoltsev[1,2], A. G. Kharlamov[1,2], A. A. Korol[1,2], S. V. Koshuba[1], D. P. Kovrizhin[1,2], A. S. Kupich[1], K. A. Martin[1,2], A. E. Obrazovsky[1], E. V. Pakhtusova[1], S. I. Serednyakov[1,2], D. A. Shtol[1,2], Z. K. Silagadze[1,2], I. K. Surin[1,2], Yu. V. Usov[1,2], and A. V. Vasiljev[1,2]
The SND Collaboration

[1] *Budker Institute of Nuclear Physics, Novosibirsk, 630090, Russia*
[2] *Novosibirsk State University, Novosibirsk, 630090, Russia*

Abstract. New results on exclusive hadron production in e^+e^- annihilation obtained in experiments with the SND detector at the VEPP-2M and VEPP-2000 e^+e^- colliders are presented.

1 Detector and experiment

The SND [1–4] is the general purpose nonmagnetic detector. Its main part is a spherical three-layer electromagnetic calorimeter containing 1640 NaI(Tl) crystals. Directions of charged particles are measured by a tracking system based on a nine-layer drift chamber. The particle identification is provided by dE/dx measurements in the tracking system and a system of aerogel Cherenkov counters. Outside the calorimeter a muon detector is located.

SND collected data at the VEPP-2M [5] and VEPP2000 [6] e^+e^- colliders. At VEPP-2M, data with an integrated luminosity of about 30 pb^{-1} were recorded in 1996-2000 in the energy range 0.4–1.4 GeV. At VEPP2000, a wider energy interval, 0.3–2.0 GeV, is studied. A 69 pb^{-1} data sample was collected during 2010-2013. Currently the VEPP-2000 accelerator complex is under upgrade. Experiments with increased luminosity are expected to be started in the end of 2016.

The main goal of the SND experiments is careful measurement of exclusive hadronic cross sections below 2 GeV, which are, in particular, needed for the Standard Model calculation of the muon $(g-2)$ and running α_{QED}. Here we present new results on measurement of four exclusive cross sections.

2 Precise cross-section measurements

The $e^+e^- \to \pi^0\gamma$ cross section is the third largest cross section (after $e^+e^- \to \pi^+\pi^-$ and $\pi^+\pi^-\pi^0$) below 1 GeV. From analysis of the $e^+e^- \to \pi^0\gamma$ data in the vector meson dominance (VMD) model, the widths of vector-meson radiative decays are extracted, which are widely used in phenomenological

⋆e-mail: druzhinin@inp.nsk.su

models. The most accurate data on this process were obtained in experiments at the VEPP-2M e^+e^- collider with the SND [7, 8] and CMD-2 [9] detectors. The SND results [7, 8] are based on about 25% of data collected at VEPP-2M. Here we present a new analysis [10] using the full SND@VEPP-2M data sample.

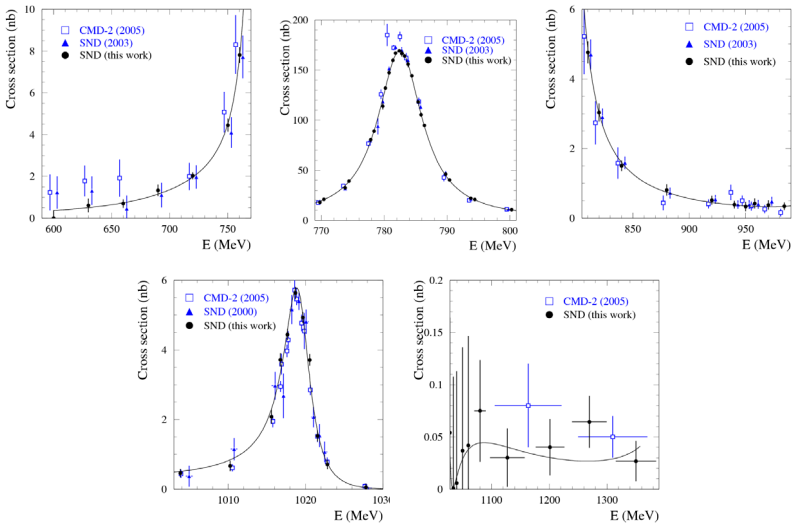

Figure 1. The $e^+e^- \to \pi^0\gamma$ cross section measured by SND using the full VEPP-2M data sample in comparison with the previous most accurate measurements. The curve is the result of the VMD fit. Only statistical errors are shown. The systematic errors are 3.2%, 3%, and 6% for SND (2000), SND (2003), and CMD-2 (2005) data, respectively. Our systematic uncertainty at the ω and ϕ peaks is 1.4%.

The measured $e^+e^- \to \pi^0\gamma$ cross section shown in Fig. 1 agrees with previous SND [7, 8] and CMD-2 [9] measurements within the systematic uncertainties, but is significantly more precise. From the fit to cross section data we obtain the products of branching fractions:

$$\begin{aligned} B(\rho \to \pi^0\gamma)B(\rho \to e^+e^-) &= (1.98 \pm 0.22 \pm 0.10) \times 10^{-8}, \\ B(\omega \to \pi^0\gamma)B(\omega \to e^+e^-) &= (6.336 \pm 0.056 \pm 0.089) \times 10^{-6}, \\ B(\phi \to \pi^0\gamma)B(\phi \to e^+e^-) &= (4.04 \pm 0.09 \pm 0.19) \times 10^{-7}, \end{aligned} \quad (1)$$

For the ω meson, we improve accuracy of the product by a factor of 1.6. There is a tension between the value of the ratio $B(\omega \to \pi^0\gamma)/B(\omega \to \pi^+\pi^-\pi^0)$ measured by KLOE [11] and the same value obtained using VEPP-2M data. After our $\pi^0\gamma$ measurement this tension increases up to 3.4σ. Our $\rho \to \pi^0\gamma$ measurement is most precise. The obtained branching fraction $B(\rho \to \pi^0\gamma) = (4.20 \pm 0.52) \times 10^{-4}$ is lower than the PDG value by 1.8σ, but agrees with the branching fraction for the charged ρ decay. The result for the $\phi \to \pi^0\gamma$ has an accuracy comparable with that of the PDG value. It is obtained in the fit, in which the relative phase between the ϕ and ω amplitudes ($\varphi_{\phi\omega}$) is taken from data on the $e^+e^- \to \pi^+\pi^-\pi^0$ process. In the fit with free $\varphi_{\phi\omega}$, $B(\phi \to \pi^0\gamma)$ is determined with about 20% uncertainty.

We also improve accuracy of $e^+e^- \to K^+K^-$ cross section measurement in the energy range 1.05–2.00 GeV [13]. Our result in comparison with most precise previous measurement by BABAR [12] is shown in Fig. 2.

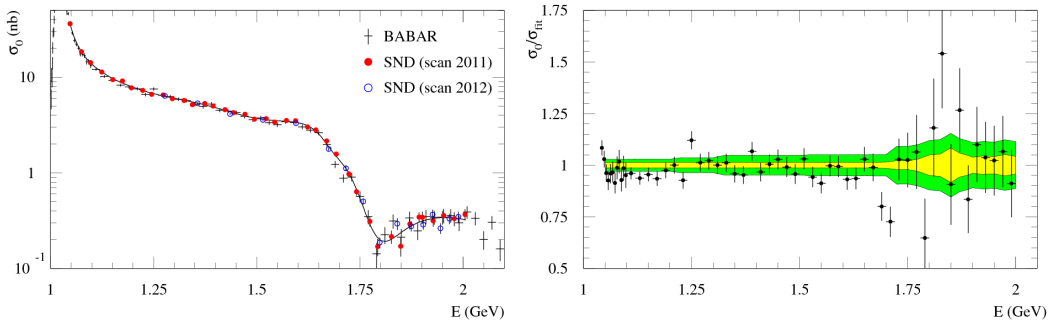

Figure 2. Left panel: The $e^+e^- \to K^+K^-$ cross section measured by SND at VEPP2000 and in the BABAR experiment [12]. The curve is the result of the VMD fit. Right panel: The relative difference between the $e^+e^- \to K^+K^-$ cross sections measured by BABAR and the fit to the SND data. The SND and BABAR systematic uncertainties are shown by the light and dark shaded bands, respectively.

3 Previously unmeasured cross sections

Relatively precise inclusive data on e^+e^- annihilation to hadrons exist above 2 GeV. Below the total hadronic cross section is calculated as a sum of exclusive cross sections. However, in the energy region between 1.5-2.0 GeV the exclusive data are incomplete. In this section we discuss two previously unstudied process.

The process $e^+e^- \to \pi^+\pi^-\pi^0\eta$ has complex internal structure. Our preliminary study show that there are at least four mechanisms for this reaction: $\omega\eta$, $\phi\eta$, $a_0(980)\rho$, and structureless $\pi^+\pi^-\pi^0\eta$. The known $\omega\eta$ and $\phi\eta$ contributions explain about 50-60% of the cross section below 1.8 GeV. Above 1.8 GeV the dominant mechanism is $a_0\rho$. The preliminary result on the $e^+e^- \to \pi^+\pi^-\pi^0\eta$ cross section is shown in Fig. 3 (left). The cross section for the subprocess $e^+e^- \to \omega\eta$ is measured separately [14] and shown in Fig. 3 (right) in comparison with the BABAR measurement [15]. Our results have better accuracy and disagree with the BABAR data at $E > 1.6$ GeV.

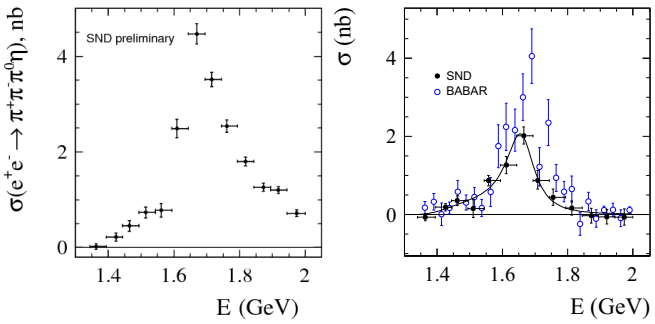

Figure 3. Left panel: The $e^+e^- \to \pi^+\pi^-\pi^0\eta$ cross section measured by SND. Right panel: The $e^+e^- \to \omega\eta$ cross section measured by SND in comparison with BABAR data [15]. The curve is the result of the VMD fit.

The process $e^+e^- \to \omega\pi^0\eta$ is studied in the seven-photon final state [16]. Events of the $e^+e^- \to \pi^0\pi^0\eta\gamma$ process are selected. The analysis of their $\pi^0\gamma$ invariant-mass distribution shows

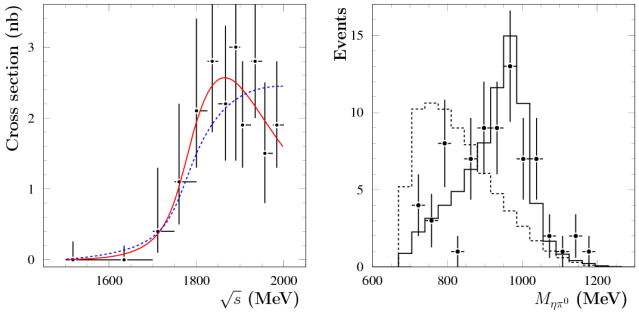

Figure 4. Left panel: The $e^+e^- \to \omega\eta\pi^0$ cross section measured by SND. The solid (dashed) curve shows the result of the fit in the model of $\omega a_0(980)$ intermediate state with (without) a resonance contribution. Right panel: The $\eta\pi^0$ invariant mass spectrum for selected $e^+e^- \to \omega\eta\pi^0$ events. The solid histogram represents $e^+e^- \to \omega a_0(980)$ simulation, while the dashed histogram represents $\omega\eta\pi^0$ phase-space simulation.

the dominance of the $\omega\pi^0\eta$ intermediate state. The measured $e^+e^- \to \omega\pi^0\eta$ cross section is shown in Fig. 4 (left). Figure 4 (right) shows the $\pi^0\eta$ mass distribution for selected $\omega\pi^0\eta$ events, which is well described by the model the of $\omega a_0(980)$ intermediate state.

Both the previously unmeasured cross sections discussed in this section give a sizable contribution ($\sim 5\%$) to the total hadronic cross section.

Acknowledgments: This work is supported in part by the RFBR grants 16-02-00327, 16-02-00014, 15-02-01037, 16-32-00542, and 14-02-00129. Part of this work related to the photon reconstruction algorithm in the electromagnetic calorimeter is supported by the Russian Science Foundation (project No. 14-50-00080).

References

[1] M. N. Achasov *et al.*, Nucl. Instrum. Methods Phys. Res., Sect. A **598**, 31 (2009)
[2] V. M. Aulchenko *et al.*, Nucl. Instrum. Methods Phys. Res., Sect. A **598**, 102 (2009)
[3] A. Y. Barnyakov *et al.*, JINST **9**, C09023 (2014)
[4] V. M. Aulchenko *et al.*, Nucl. Instrum. Methods Phys. Res., Sect. A **598**, 340 (2009)
[5] I. A. Koop *et al.*, in *Proceedings of the Workshop on Physics and Detectors for DAPHNE*, Frascati, Italy, 1999 (Frascati, 1999), p. 393
[6] A. Romanov *et al.*, in *Proceedings of Particle Accelerator Conference PAC 2013, Pasadena, CA USA, 2013*, p. 14
[7] M. N. Achasov *et al.* (SND Collaboration), Eur. Phys. J. C **12**, 25 (2000)
[8] M. N. Achasov *et al.* (SND Collaboration), Phys. Lett. B **559**, 171 (2003)
[9] R. R. Akhmetshin *et al.* (CMD-2 Collaboration), Phys. Lett. B **605**, 26 (2005)
[10] M. N. Achasov *et al.* (SND Collaboration), Phys. Rev. D **93**, 092001 (2016)
[11] F. Ambrosino *et al.* (KLOE Collaboration), Phys. Lett. B **669**, 223 (2008)
[12] J. P. Lees *et al.* (BaBar Collaboration), Phys. Rev. D **88**, 032013 (2013)
[13] M. N. Achasov *et al.* (SND Collaboration), arXiv:1608.08757 [hep-ex]
[14] M. N. Achasov *et al.* (SND Collaboration), arXiv:1607.00371 [hep-ex]
[15] B. Aubert *et al.* (BABAR Collaboration), Phys. Rev. D **73**, 052003 (2006)
[16] M. N. Achasov *et al.* (SND Collaboration), Phys. Rev. D **94**, 032010 (2016)